Hydrology and
Earth System
Sciences

Open Access

Discussions

Sediment yield model implementation based on check dam infill stratigraphy in a semiarid Mediterranean catchment

G. Bussi[1,*], X. Rodríguez-Lloveras[2], F. Francés[1], G. Benito[2], Y. Sánchez-Moya[3], and A. Sopeña[3]

[1]Research Institute of Water and Environmental Engineering (IIAMA), Universitat Politècnica de València, Spain
[2]Geology Department, National Museum of Natural Sciences – CSIC, Madrid, Spain
[3]Geoscience Institute, CSIC, UCM, Madrid, Spain

[*]*Invited contribution by G. Bussi, recipient of the EGU Outstanding Student Poster (OSP) Award 2012.*

Discussion Paper | Discussion Paper | Discussion Paper | Discussion Paper

HESSD

10, 3427–3466, 2013

Sediment yield model implementation

G. Bussi et al.

Title Page

Abstract	Introduction
Conclusions	References
Tables	Figures

| ◄◄ | ►► |
| ◄ | ► |

| Back | Close |

Full Screen / Esc

Printer-friendly Version

Interactive Discussion

Abstract

Soil loss and sediment transport in Mediterranean areas are driven by complex non-linear processes which have been only partially understood. In order to facilitate the comprehension of these phenomena, distributed models can be very helpful tools for sediment yield estimation. In this work, a modelling approach is proposed to reproduce and evaluate erosion and sediment yield processes in a Mediterranean catchment (Rambla del Poyo, Valencia, Spain). Due to the lack of sediment transport records for model calibration and validation, a detailed description of the alluvial stratigraphy infilling a check dam that drains a $12.9\,km^2$ sub-catchment was used as an indirect evidence of sediment yield data. These dam infill sediments showed evidences of at least 15 depositional events (floods) over the time period 1990–2009. The TETIS-SED model, a distributed conceptual hydrological and sediment model, was coupled to the Sediment Trap Efficiency for Small Ponds (STEP) model for reproducing reservoir retention, and it was calibrated and validated using the sedimentation volume estimated for the depositional units associated with discrete runoff events. The results show relatively low net erosion rates compared to other Mediterranean catchments ($14\,t\,km^{-2}\,yr^{-1}$), probably due to the extensive outcrops of limestone bedrock and rather homogeneous vegetation cover, and confirms the ephemeral behaviour of the stream. The modelled sediment production rates offer satisfactory results, further supported by palaeohydrological evidences, showing its great potential for the quantitative analysis of sediment dynamics in ungauged Mediterranean basins.

1 Introduction

Modelling sediment yield is a complex task due to non-linearity of natural processes intervening at slope and basin scale (Schumm and Lichty, 1965; Coulthard et al., 1998; Roering et al., 1999). Recent computing advances, together with a better understanding of hydrodynamic processes involved in the surface runoff, sediment production

and sediment transport, have stimulated the development of physically based and distributed parameter models (e.g. WEPP, EUROSEM and LISEM). The reliability of such sediment yield models depends on a robust calibration-validation process that, in ungauged catchments, as it is the case of most of small semiarid basins around the world,

5 may limit a broad use of such distributed sediment cycle models. Different authors have used the sediment volume accumulated in lakes and reservoirs as an indirect validation method for modelling sediment yield at the regional scale (Van Rompaey et al., 2003; Grauso et al., 2008). Reservoir sediment volume has been used since the 1950s as an estimate of the catchment mean sediment yield for comparison with the results of em-

10 pirical equations (ICOLD, 1989; Avendaño Salas et al., 1995). However, this technique was not extensively employed until the 1980s (Jolly, 1982; Le Roux and Roos, 1982; Duck and McManus, 1993). As an example, Avendaño Salas et al. (1997) carried out bathymetries at different years on 60 reservoirs distributed throughout Spain, creating a reservoir sedimentation dataset which they later analysed. Verstraeten et al. (2003)

15 also estimated long-term sediment yield starting from this dataset.

Recently, sediment volumes stored in water-retention dams have also been used for distributed mathematical model validation, as showed in De Vente et al. (2005), De Vente et al. (2008) and Alatorre et al. (2010). In De Vente et al. (2005), two semi-quantitative models for mean annual net erosion rates estimation are compared, and

20 their results contrasted versus reservoir sedimentation rates. In De Vente et al. (2008), the reservoir sedimentation rates were used to compare the results of three distributed approaches for soil erosion rates and long term sediment yield estimation: the WA-TEM/SEDEM model (Van Rompaey et al., 2001), the PESERA model (Kirkby et al., 2008) and the SPADS model (De Vente et al., 2008). In Alatorre et al. (2010), the WA-

25 TEM/SEDEM model is calibrated using the depositional record of the Barasona reservoir (NE Spain) and then used for Ésera River catchment sediment yield modelling, providing mean annual erosion and sediment yield.

Not only large reservoir deposits, such as the Spanish dataset mentioned above (Avendaño Salas et al., 1997), can be used for model calibration and validation, but

also smaller reservoirs like check dam reservoirs, irrigation and water supply reservoirs, etc., can be a source of information in a similar way. Verstraeten and Poesen (2000) quantify the number of these structures around the world in a few million, with small dams being defined as retention structures with a storage capacity of between 50 and 5×10^6 m³. The large number of small reservoirs in the world means that there is a high potential for sediment yield assessment and modelling. Some examples of sediment yield studies based on sedimentation volumes in small reservoirs include McManus and Duck (1985), Van den Wall Blake (1986), Neil and Mazari (1993), Foster and Walling (1994), White et al. (1996), Romero-Díaz et al. (2007), Boix-Fayos et al. (2008), Sougnez et al. (2011) and Bellin et al. (2011). Verstraeten and Poesen (2002) calculated the error on sediment yield estimation for 21 catchments located in central Belgium using small reservoir deposits and concluded that this is a suitable methodology for medium-sized catchments (10^1–10^4 km²) and for mid-term sediment yield estimations (10^0–10^2 yr). Errors on topographical surveys, sediment dry bulk density and reservoir trap efficiency must be taken into account, although the mean accuracy of this technique is comparable to other methodologies used for sediment yield estimation such as sediment rating curves or suspended sediment sampling.

Reservoir sedimentation rates are a very helpful tool for estimating catchment sediment yield, but indeed this methodology has some weaknesses: (i) the quality of the reservoir storage capacity estimation is sometimes questionable, especially for the starting reservoir capacity (when the reservoir was built); (ii) the calculated sediment yield is averaged over a large time (Alatorre et al., 2012); (iii) the total deposition volume does not give information about temporal patterns (event sediment production) and their variability. In the case of large reservoirs and artificial lakes, sediment coring and paleolimnological techniques including geochronological dating (Cs-137, Pb-210) have been used for temporal characterisation of sediment rates (e.g. artificial Lake Matahina by Phillips and Nelson, 1981; Brno reservoir in Czech Republic by Nehyba et al., 2011).

In Mediterranean ephemeral streams a large number of check dams have been built to prevent or reduce sediment inputs into perennial streams during the first winter or rainy season following a wildfire (Boix-Fayos et al., 2008) or to correct local channel slope (Romero-Diaz et al., 2007). In these check dams, infill deposits record pulses of sediments produced during discrete flood events. The coarse texture of the deposited material prevents from coring but allows the use of fluvial palaeohydrological techniques. The detailed analysis of their alluvial stratigraphy may provide quantitative information for specific events, such as the number of events, timing, and deposited volume(s) of an individual flood or floods. Similar techniques have been used in the reconstruction of the magnitude and frequency of past floods using geological evidence (Kochel and Baker, 1982; Baker, 2008; Benito et al., 2010; Machado et al., 2011).

In this work, the distributed TETIS model is used to reproduce the hydrological (Francés et al., 2002, 2007) and sediment regime (Montoya, 2008) of a small semi-arid Mediterranean Basin (Rambla del Poyo, Valencia, Spain). Measured water discharge is used to calibrate the hydrological sub-model; the sedimentation of a small reservoir, draining a 12.9 km^2 subcatchment, is used to calibrate the sediment sub-model. Time-variable trap efficiency is taken into account by coupling the STEP model (Verstraeten and Poesen, 2001) with the TETIS model, while dry bulk density is calculated by Lane and Koeltzer formulae (Lane and Koelzer, 1943). The sediment yield temporal validation is carried out by comparing the model output with the results of a stratigraphical description (unit thickness, minimum sediment volume, texture) of depositional sequences observed in two trenches dug across the reservoir sediment infill. The sedimentary infill shows evidence of 15 floods events that occurred following the dam construction in 1992 up to year 2009. A date is assigned to each flood unit based on layers containing anomalous high charcoal accumulation due to well documented historical wildfires.

2   Materials and methods

2.1   The TETIS model

The TETIS model is a distributed, conceptual model for hydrology, erosion and sediment cycle simulation. It is formed by a hydrological sub-model and a sediment sub-model.

The hydrological component of TETIS has been already presented in many literature works, such as Francés and Benito (1995), Francés et al. (2002), Francés et al. (2007), Morales de la Cruz and Francés (2008) and Vélez et al. (2009). Each cell of spatial grid is represented as five connected tanks, as shown in Fig. 1. The connections between tanks are represented as linear reservoir relations and flow threshold schemes.

The first tank (T1) corresponds to the sum of the soil capillary retention, surface and vegetation interception and it is called static storage; its only exit is evapotranspiration. The second tank (T2) reproduces the surface water, i.e. the part of precipitation which generates overland flow. The third tank (T3) corresponds to the gravitational storage of the upper soil; it generates the interflow. The fourth tank (T4) corresponds to the aquifer, which produces base flow. The percolation process is modelled according to both soil saturation conditions and vertical hydraulic conductivity, and the remaining water in T3 is available to feed the interflow. The last tank (T5) represents the gully and river storage, i.e. the stream network storage. The flow routing in the stream network is carried out by the Geomorphologic Kinematic Wave methodology, employing nine geomorphologic parameters obtained from power laws (Francés et al., 2007) and estimated by geomorphologic regional studies. The TETIS hydrological component also includes an automatic calibration module based on the SCE-UA algorithm (Duan et al., 1992, 1994). The automatic calibration of the hydrological parameters is carried out such that up to nine correction factors (called CFs) are adjusted to fit the observed hydrographs; CFs globally correct the parameter maps (static storage, hydraulic conductivity of different soil layers, and surface and channel flow velocities), reducing the number of variables to be calibrated (Francés and Benito, 1995; Francés et al., 2007).

The TETIS sediment component was implemented by Montoya (2008) and it is based on the same conceptualization as the CASC2D-SED model (Johnson et al., 2000; Ogden and Heilig, 2001; Rojas, 2002). The conceptualization is based on the balance between sediment availability and flow transport capacity. Fine sediment transport is limited by sediment availability while coarse material transport is limited by flow transport capacity (Julien, 2010). The TETIS model divides sediment flow into three textural classes (sand, silt and clay), assigning to each of them an average diameter and a settling velocity.

The hillslope sediment erosion and transport processes are described by means of the Kilinc and Richardson equation (Kilinc and Richardson, 1973) for the total transport capacity. The sediment discharge per unit width in terms of weight is given by:

$$q_h = \alpha \, S_o^{1.66} \left(\frac{Q}{W}\right)^{2.035} \quad [\mathrm{t\,m^{-1}\,s^{-1}}] \tag{1}$$

where Q $[\mathrm{m^3\,s^{-1}}]$ is the cell overland discharge, W [m] is the cell width, S_o is the terrain slope $[\mathrm{m\,m^{-1}}]$ and α a dimensional and empirical parameter (around 25 000 for sandy bare soil with the expressed units). This equation has been modified by Julien (1995) in order to consider land use, cropping management and soil characteristics. The modified equation is the following:

$$Q_h = \frac{1}{\gamma_s} W \, \alpha \, S_o^{1.66} \left(\frac{Q}{W}\right)^{2.035} \frac{K}{0.15} \, C \, P \quad [\mathrm{m^3\,s^{-1}}] \tag{2}$$

where γ_s is sediment specific weight $[\mathrm{t\,m^{-3}}]$, K, C and P are the USLE (Wischmeier and Smith, 1978) soil erodibility, cropping management and support practice factors [–], respectively. Notice that 0.15 is the K value for sandy soil. Q_h is divided into three parts, depending on the textural composition of the transported material, and each transport capacity part is used to route downstream the corresponding soil textural class of suspended sediment. If there is residual capacity, the deposited sediments are mobilized;

if there is still residual transport capacity, the parental material is eroded. In the downstream cell, the sediments are separated into suspended or deposited depending on their settling velocity.

The stream network erosion and transport processes are described by the Engelund and Hansen equation (Engelund and Hansen, 1967), where the transport capacity depends on hydraulic radius, flow velocity, friction force and grain characteristics. The maximum sediment concentration is given by:

$$C_{w,i} = \beta \left(\frac{G}{G-1}\right) \frac{V S_f}{\sqrt{(G-1)gd_i}} \sqrt{\frac{R_h S_f}{(G-1),d_i}} \quad [-] \tag{3}$$

where G is sediment specific gravity [–], V the flow velocity [m s^{-1}], S_f the energy slope [–], g the gravity acceleration [m s^{-2}], d_i the grain diameter of textural class i [m], R_h the hydraulic radius [m] and β is a nondimensional calibration coefficient (not existing in the original expression). So, the streamflow transport capacity for the textural class i is expressed as follows:

$$Q_{s,i} = \frac{Q \ Cw_i}{\gamma_s} \quad [\text{m}^3 \text{s}^{-1}] \tag{4}$$

where Q is the stream channel discharge [m^3 s^{-1}]. Sediments are routed downstream following the same scheme as for hillslope processes. However, stream network parental material is not considered (i.e. river bed erosion or bank erosion), because in many cases the most relevant source of channel sediments are deposits left by previous floods (Piest et al., 1975), which can be introduced as initial conditions in the model. In any case, parental material can be simulated as a large sediment deposit at the beginning of the simulation. The calibration of the sediment sub-model is carried out by adjusting the α and β values.

In order to compute the effects of small retention structures such as check dams on the sediment transit, the problem of estimating trap efficiency was taken into account.

For large reservoirs, empirical formulae such as Brown (1943) or Brune (1953) can provide very likely values, especially if the reservoir trap efficiency is close to 100 % (Hu et al., 2009). Nevertheless, the uncertainty in calculating sediment trap efficiency is higher for smaller reservoirs. Moreover, trap efficiency decreases when deposition takes place and this phenomenon it is not taken into account by empirical formulae. For this reason, theoretical models have been developed to predict trap efficiency; a review can be found in Verstraeten and Poesen (2000). In this study, TETIS was coupled with the Sediment Trap Efficiency for Small Ponds model (STEP, Verstraeten and Poesen, 2001). STEP is a physically based model of the reservoir water and sediment dynamics, which can predict both long term and short term trap efficiency of small reservoirs. The model divides the reservoir into several volumes and routes the water and sediment through them using mass balance equations. In the TETIS model, the STEP model was implemented as a subroutine for on-line running, i.e. the input water and sediment discharges for STEP model are provided by the TETIS model, and the deposited volume is updated in each time-step, as well as the corresponding reservoir depth.

2.2 The study area

The study area is the Rambla del Poyo catchment, a Mediterranean ephemeral stream located 30 km west of Valencia (Spain), as showed in Fig. 2.

The geology consists of dolomites and limestones in the headwaters and marls in the lower part of the catchment (Camarasa and Segura Beltrán, 2001). The mean annual precipitation is 450 mm and the mean annual evapotranspiration is 1100 mm. The Rambla del Poyo catchment at the stream gauge station has a 184 km^2 area (Fig. 2). The upper part, or headwater, located at west, is formed by high slopes and reliefs up to 1080 m a.s.l.; nowadays, due to past wildfires, the land cover comprises mainly shrublands (*matorral*) with a little portion of pine forest. The sub-catchment drained by the check dam, which will be analysed later on (the grey area in Fig. 2), belongs entirely to this catchment portion. The land use of intermediate part is mainly formed by

non-irrigated arable land with complex cultivation patterns and transition zones. There is high presence of terraced fields. The catchment lower part is dominated by agricultural land with alternation of urban zones and periurban agriculture, mainly horchards and citrus (Salazar et al., 2012). The soils are mostly silty in the upper and intermediate part of the catchment, and clayey in the lower part. The stream network is composed by four major water courses: the Barranco Grande at the north, the Barranco de Ballesteros and the Barranco de la Cueva Morica at the centre and the Barranco del Gallo at the south.

Soil data for estimating hydrological and sedimentological model parameters was mainly taken from LUCDEME project (Rubio et al., 1995). Using soil profiles, texture information and pedotransfer functions (Saxton and Rawls, 2006), the static storage and the hydraulic conductivity of the upper soil were estimated (Fig. 3). C and K USLE factors were taken from a previous work (Antolín, 1998), and are also shown in Fig. 3. The P factor of the USLE was set to 1, since no support practice is used.

The effect of two wildfires that occurred in 1994 and 2000 was taken into account by modifying the C USLE factor during a "windows of disturbance" (as defined by Prosser and Williams, 1998) after the fires. Within the burnt zones (the extension of both fires was provided by the Valencia Regional Government, Wildfire Management Service), the vegetation cover and management factor (C) was set to high values, since vegetation in burnt areas was almost absent (similarly to what was done by Rulli et al., 2005). The length of the windows of disturbance was chosen following Andreu et al. (2001), so that the highest susceptibility to soil erosion of burnt areas takes place at the first severe rainfall event after one wildfire, usually on autumn – winter (Shakesby, 2011). As demonstrated by Campo et al. (2006) for a plot located close to the Rambla del Poyo catchment, this effect seriously increases the soil erosion, especially when a severe rainfall occurs a few days or weeks after the wildfire.

A stream gauge, located at the basin outlet, and a raingauge, located at the same place, provide 5 min resolution discharge and precipitation series; the available data start from 1988.

2.3 The check dam

Indirect evidence of sediment production at the study area was provided by sediments stored on a small concrete check dam (Fig. 4) built in 1992 and draining a catchment area of 12.9 km^2. The reservoir maximum storage volume is 3000 m^3, and at the time of the field survey was about half of its total volume capacity. This dam was chosen for its high siltation rate and for its accessibility.

A field study was carried out to survey the dam body and to describe the infill flood stratigraphy including collection of sediment samples for textural analysis of the sedimentary sequences. A topographic survey was also carried out at the sedimentation area and the surrounding slopes with a real time kinematic differential GPS topographic survey, in order to better estimate the deposited volume.

Two trenches were dug across the reservoir sedimentation infill, at 9.5 m and 22 m from the dam respectively, called BG-1 and BG-2 (Fig. 5). Detailed stratigraphic panels were carried out using a one meter side vertical grid over the trench, where stakes with reference numbers were put at regular intervals. In these panels all the depositional contacts were traced laterally, with emphasis on breaks that indicate sedimentary interruption and post-flood surface exposure. The panels allowed a better detection of lateral interfingering beds, potential erosion and depositional gaps. Correlation between these two panels was possible due to anomalous charcoal content of some reference alluvial beds. Sediment samples for each unit were collected for determination of organic matter and micro-charcoal content (as indicator of fires) and for a complete textural analysis.

Starting from the reservoir geometry, the GPS survey and the flood unit morphology, the volume of each alluvial layer deposited by an individual flood was estimated by using two different methodologies: (i) "wedge" approach: given the layer depths inside the trenches, the sedimentation length and the distance between trenches, every layer volume was calculated as if each flood unit had a pyramidal shape (such as a wedge); (ii) proportional approach: given the surface shape and the layer depths inside the

trenches, each layer volume was estimated by subtracting to the actual deposits the average accumulated layer depth, considering the thickness difference of each layer in each trench and approaching it to a pyramidal shape.

3   Results and discussion

3.1   Hydrological calibration and validation

The first step of this work was the calibration and validation of the TETIS hydrological sub-model. It is proven that, in Mediterranean climate, only a few events scattered over a large time period are responsible for most of the total sediment load (Gallart et al., 2005). Given that the aim of this study is the sediment yield modelling, calibration and validation focused on the reproduction of heavy rainfall events. The model was calibrated at a 5 min time resolution on a single event in October 2000, by means of the TETIS automatic calibration algorithm and validated on 37 rainfall event from 1990 to 2009. Since the simulation of 20 yr of rainfall at 5 min time resolution is highly time-costing, a continuous simulation with variable time step was used: first, a time period preceding the first rainfall event of the series (the first no flood period) was simulated with a daily time step; second, the final soil moisture state was used as initial state for the first event, simulated with a 5 min time step; then, the final state of the first event was used as initial state of the second no flood period, and so on, concatenating 38 no flood and 38 flood events. Thus, a daily model had to be calibrated and validated before starting the 5 min calibration procedure. Its results are shown in Fig. 6. The calibration (October 2000 to October 2003) gave a Nash–Sutcliffe index (NSE, Nash and Sutcliffe, 1970) equals to 0.82, and the validation (from 1998 to 2010 excluding the calibration period) provided a 0.72 NSE index, giving a very good daily calibration and a good daily validation, following the performance classification given by Moriasi et al. (2007).

Using the initial soil moisture given by the daily model simulation, the 5 min model automatic calibration was carried out. The simulated hydrograph is shown in Fig. 7

(left). The obtained NSE index is 0.78, with a volume error of −10 %, which can be considered very good, following Moriasi et al. (2007). The temporal flood validation also provided good results. In Fig. 7 (right) the January 1998 event is shown. For this event, the NSE index is 0.5 and the volume error is 24 %; this validation result can be judged as satisfactory, given that, although there is a shift between the observed and simulated peaks, due to a poor description of the rainfall spatial distribution, the hydrograph shapes are very similar, and the peak discharge error, which is very relevant when modelling sediment yield, is relative small (15 %). For other flood events, the model also obtains acceptable performances in terms of volume error, peak discharge error and hydrograph visual fit. The model also reproduces satisfactorily the ephemeral behaviour of the catchment; the base flow is absent, and the channel flow is composed mainly by overland flow with a little contribution of interflow (for heavy flood events, only 0.1 % of total flow), which is in accordance with our prior catchment hydrological knowledge. The model tends to provide a good estimation of the high peak flows, while the error on small intensity events is greater, probably due to the high uncertainty on the spatial distribution of the precipitation (only one pluviograph, located at the gauge station, was available for the whole catchment). The initial soil moisture estimation by warm up simulation period at the daily scale has been proven to be suitable, although some small error can be detected, as for example in the Fig. 7 – left, where the first peak of the flood is underestimated, probably due to an underestimation of initial soil moisture.

3.2 Alluvia infill volume estimation

The geometry of the dam alluvial infill can be described as a sedimentary wedge with a triangular plan view (Fig. 8). The active channel is bordering the right margin of the reservoir area, partially undercutting the slope deposits. In the upper-mid reach of the reservoir the most relevant morphosedimentary feature is a lateral gravel bar (43 m in length) attached to the left valley side, with a prominent 1-m high frontal scarp, indicating a progradation over the fine deposits located closer to the dam. This alluvial

bar is composed by poorly sorted gravels and boulders in a matrix of sand and silt, with a lack of structure, suggesting a deposition by flash flow(s) associated with detrital heavy load and loss of energy due the slope reduction caused by the previous dam infill. Closer to the dam wall, the alluvial infill comprises a 2.5-m thick deposit composed by multiple layers of well sorted sands and silts with ripples, planar and cross-bedded lamination and parallel lamination. The geometry of the layers is horizontal close to the reservoir centre but increases its elevation and decreases its thickness towards the valley side.

Two trenches were dug across the check dam sedimentation infill. The first trench (BG-1: Figs. 4 and 8) is about 10 m in length, covering from the left valley side to the main channel at the right margin, by 2.5 m in depth exposing sequences of multiple fine-grained flood deposits linked to the development of an eddy flow behind of the over-elevated left part of the dam wall. The stratigraphic sequences found in BG-1 (Fig. 9) provide evidence of at least 15 individual floods units post-dating the dam, as the dam infill fine sediments overlay old slope and stream channel gravels (Fig. 8). The lower seven flood units suggest a period of relatively small floods, on the basis of the very fine and fine sand grain size and thin stratigraphic layers. The upper part of the sequence is represented by eight flood layers of medium to coarse sand within units of 20 to 60 cm in thickness with parallel and planar cross-stratification indicating a higher energy and sediment load than the lower flood units. The flood units 3 to 10 contain a large amount of charcoal debris concentrated on distinct 1–2 cm thick laminae, which were probably deposited after severe wildfires that occurred in 1994 and 2000.

The second trench (BG-2, Fig. 8) is about 8.5 m long by 2 m deep, and it was excavated across the reservoir infill 12.5 m upstream of BG-1. In the lower 1-m section, at least eight flood units were distinguished and correlated with the lower ten flood units in BG-1, with exception of units 5 and 8 that pinched out at some point between both trenches (Fig. 8). The upper one meter of BG-2 is composed by gravels with cross-bedding at the base and massive non-structured at the top, the latter being the frontal lee face of the lateral gravel bar described previously. The relationship of these gravels

with the fine-grain deposits of BG-1 is not obvious and either the gravels are the proximal facies of the floods that deposited units 11 to 15 in BG-1, or they corresponds to a later large magnitude flood whose coarse sediments are prograding over the upper five units in BG-1. However, the lack of stratigraphic breaks in the gravel unit prevents a detail correlation with the last five events described in BG1, and for practical purposes the gravel volume was considered as a sum of the last five events described in BG1. A complete textural analysis was carried out for each flood unit in BG-1, showing that sediments are mainly composed by sand, whose percentage varies between 77 and 99 %. The dry bulk density of the infill deposits was estimated in 1.195 t m^{-3} using the approach suggested by Lane and Koelzer (1943) based on textural data and coefficients for dry reservoirs.

3.3 Sediment sub-model calibration and validation

The TETIS sediment sub-model was first calibrated using the total sediment volume accumulated behind the check dam. The variability in time of the reservoir trap efficiency was taken into account by the STEP approach. The reservoir was divided into 10 finite volumes and the reservoir routing time-step was 1 s; the incoming water and sediment discharges were calculated by means of TETIS model. The input sediment yield was divided into three textural classes (sand, silt and clay), and a reservoir settling velocity value was assigned to each particle size, following Julien (1995). The calibration was carried out by trial and error adjusting the values of α (for hillslopes) and β (for stream channel network) coefficients within a range of feasible values, following the modellers' expertise. The objective function used in this calibration process was the total volume error expressed in percentage. The best value of the objective function (i.e. 0 %) was provided by the parameter set $\alpha = 350$ and $\beta = 0.05$.

Then, the simulated sediment yield and deposited sediment series were analysed for model validation. As shown in Fig. 10, the simulated depositional sequence shows the predominance of seven flood events, which account for the 86 % of the total simulated deposits of the check dam reservoir for the time period 1990–2009. For the sediment

Full Screen / Esc

Printer-friendly Version

Interactive Discussion

regime reconstruction, a date of occurrence was assigned to the flood units described in the stratigraphy considering (1) the relative stratigraphic order of layers since dam construction in 1990, (2) largest rainy events were more probable to produce the largest sediment yields, and moreover (3) sedimentary units containing 1–2 cm charcoal debris lamina were deposited during rainfalls following wildfire events.

Two major wildfires affected the check dam catchment since early '90s, dating summer 1994 and 2000, and the first floods following the fires took place in December 1995 and October 2000. Lamina with high content of charcoal debris was detected in layer 3 and 9, with decreasing concentration on the overlying beds. Hence, the flood unit 3 was related to the December 1995 flood event and the flood units 1 and 2 to the previous two floods (December 1992 and April 1994). As a partial confirmation of this statement, the flood unit 3 is one of the thickest layers, and following the hydrological model results, the December 1995 flood event had the second highest peak discharge of the simulated series (1990–2009). Flood units 4 to 7 were assigned to four consecutive minor flood events (January 1996, January 1997, January 1998 and July 1999, respectively). Flood units 8, 9 and 10 were all related to October 2000 flood event; in fact, this flood event presented three peaks (Fig. 7 – left), and for this reason, deposited three flood units. Flood units 11 to 15 were related to the following 5 flood events (April 2001, May 2002, September 2003, November 2006 and April 2007). The upper layer of undistinguished sediments (the surface gravel body) was assumed to be produced by the last three flood events of the time series (October 2007, October 2008 and September 2009).

Following the previous chronological assumptions on the dam alluvial stratigraphy, the sediment volume estimated for each flood units (i.e. the observed volume of each layer) and the simulated volume provided by the model were compared (Fig. 11). As the temporal validation in Fig. 11 shows, the results are reasonably acceptable giving the high uncertainty of the silting process, showing a volume error between −80 % and 80 % for the most relevant events. Nevertheless, it is clear that the model tends to overestimate the observed values, especially for the high magnitude events. Since the

Full Screen / Esc

Printer-friendly Version

Interactive Discussion

model was calibrated using the total volume deposited in the reservoir, the overestimation is compensated by the underestimation of the remaining sedimentation volume; i.e. the gravel and sand massive deposit on BG-2, with an error of −66 %. This error is probably due to an incorrect reproduction of the sediment reservoir dynamics when the reservoir filling overcomes a certain level. In this case, the conditions for fine alluvial deposition are not fulfilled anymore, and erosion and mixing processes take place. The STEP model does not take into account these phenomena, since it only considers sediment deposition.

In order to overcome this problem, the model was finally calibrated using the period 1992–2007; in this way, the simulated period does not cover the last years, when STEP model it is not reproducing correctly the reservoir dynamics. The results show a better agreement between the estimated and the simulated volumes, as shown in Fig. 12. The resulting parameters were $\alpha = 268$ and $\beta = 0.05$.

The model performance can be described as satisfactory, since the volume error for the deepest flood unit is included between −50 and 50 %, which, considering the high uncertainty involved in the modelling process can be considered a positive result. This statement confirms that small check dams can be a very important source of information for modelling calibration and validation, and shows that palaeoflood techniques can help improving model performance and calculating sediment yield both for long and short term.

3.4 Sediment yield

The simulated texture of deposited sediments is sandy (between 87 % and 100 % of sand), agreeing with the field measurements. This result partly proves the correct operation of the STEP model for trap efficiency computation. The model provided an average sediment trap efficiency of 51 %, ranging from 29 % to 100 %. The trap efficiency varies depending on the flood magnitude and the reservoir capacity, which changes in time, along with the reservoir filling. Giving the annual average simulated flow ($2.05\,\mathrm{Mm}^3$) and the reservoir storage capacity ($3000\,\mathrm{m}^3$), the Brune curves

(Brune, 1953) provide a trap efficiency value ranging between 44 % and 68 %, with a median of 57 %, which is reasonably close to the value provided by the model. On the other hand, the Brown equation (Brown, 1943), used in Bellin et al. (2011) and in Boix-Fayos et al. (2008), provides a lower value, equal to 33 %.

The resulting average specific sediment yield (SSY) at the catchment is 13.6 t km^{-2} yr^{-1}. Given an inter-annual average value of trap efficiency, Bellin et al. (2011) proposed the following formula for calculating area-specific sediment yield (t km^{-2} yr^{-1}):

$$SSY = \frac{100\gamma V}{AY\text{TE}} \tag{5}$$

where γ is the mean bulk density (t m^{-3}) of the deposited sediment, V is the estimated volume of trapped sediment (m^3), A the drainage area (km^2), Y the period over which sediment has accumulated (years), and TE the trap efficiency (%). Using the sediment trap efficiency value provided by the model and the density calculated above, the SSY provided by Eq. (5) is 13.7 t km^{-2} yr^{-1}, which is very similar to the value obtained by the model. However, SSY can be misleading, especially in a Mediterranean catchment, due to the high interannual variability of runoff and sediment yield. In fact, the model results suggest that annual sediment yield varies between 0.32 t km^{-2} for the year 2004 and 116.82 t km^{-2} for the year 2000.

These SSY values are slightly lower than the ones obtained in similar works in Spanish Mediterranean catchments, as González-Hidalgo et al. (2007), Romero-Díaz et al. (2007), Bellin et al. (2011) and Sougnez et al. (2011), or in the Spanish Pyrenees areas (Bathurst et al., 2007) although those works were carried out in more erosion-prone catchments. No degraded areas such as marl gullies or badlands are present in the Rambla del Poyo catchment, mainly because the dominant rock is the limestone with significant areas of outcrops, and the vegetation cover is rather homogeneous and denser than other Mediterranean areas studied in the previously cited studies (mostly located in more arid areas such as the SE of Spain).

The greatest flood event, in terms of peak flow and sediment yield, was the October 2000 flood, which accounted for the 40 % of the total deposited volume and the 43 % of the total sediment yield of the check dam sub-catchment. The SSY for this event was 116 t km^{-2}, a high sediment yield value for shrubland catchments. The trap efficiency was 35 %. The most important four events accounted for the 80 % of the total sediment yield, and the most relevant eight for the 90 %. This phenomenon, which has been noticed in many ephemeral streams (Gallart et al., 2005), is due to the rainfall regime, which is characterized by long dry periods and heavy and short bursts, and the well-known highly non-linear relationship between water discharge and sediment yield.

4 Conclusions

Deposits stored in check dams are a direct evidence of sediment produced at the upstream catchment, for both short (event scale) and long term (since dam construction). Mean annual sediment yield can be calculated from the total volume of sediment retained behind the check dams, as done by Bellin et al. (2011) and Sougnez et al. (2011). This paper shows that a distributed sediment model can be implemented using the proxy information obtained from check dam deposits. The model implementation considered not only the total volume retained in the check dam for calibration, but also volumes associated with individual flood layers for validation. Detailed alluvial stratigraphy was analysed in two parallel trenches (12.5 m apart) across the dam infill. At least 15 flood layers associated to single flood or flood pulses were identify based on evidences of aerial exposure of sediment contacts (e.g. mudcracks and rootmarks). These palaeoflood sedimentary units were traced along the trenches and correlations between the layers found at the two trenches were established on the basis of key beds containing charcoal debris or dark mud. A detailed differential GPS survey together with the thickness and geometry of individual flood layers provided a total estimated accumulation volume that were deposited over the time period 1990–2009.

The TETIS sediment yield sub-model was calibrated using the total sediment volume accumulated in the check dam infill. The variability in time of the reservoir trap efficiency was taken into account by coupling the TETIS and the STEP models. The simulated results show good agreement with the estimated sediment volumes retained behind the check dam, both at short and long term. The model provides a specific sediment yield of $14\,\mathrm{t\,km^{-2}\,yr^{-1}}$ for a $12.9\,\mathrm{km^2}$ sub-catchment of Rambla del Poyo, which is lower than other net erosion rates recorded or estimated in the east of Spain, probably due to extensive limestone bedrock outcrops, thin soils and dense vegetation cover (shrublands with a little portion of pine forest). The model confirms the ephemeral behaviour of the stream, and the Mediterranean character of the sediment yield, mainly associated to flow pulses during a limited number of storm events. Almost 90 % of total deposited volume behind the check dam is due to only 8 events in 20 yr, and the 80 % of total volume to 4 flood events. The greatest flood event (October 2000) account for the 40 % of the total deposited volume and the 43 % of the total sediment yield, following model results. The trap efficiency, calculated by the STEP model, varies depending on the magnitude of the flood event and on reservoir filling, from around 30 % for the first rainfalls of the simulated series to 55–60 % for the most recent flood events.

References

Alatorre, L. C., Beguería, S., and García-Ruiz, J. M.: Regional scale modeling of hillslope sediment delivery: a case study in the Barasona Reservoir watershed (Spain) using WATEM/SEDEM, J. Hydrol., 391, 109–123, doi:10.1016/j.jhydrol.2010.07.010, 2010.

Alatorre, L. C., Beguería, S., Lana-Renault, N., Navas, A., and García-Ruiz, J. M.: Soil erosion and sediment delivery in a mountain catchment under scenarios of land use change using a spatially distributed numerical model, Hydrol. Earth Syst. Sci., 16, 1321–1334, doi:10.5194/hess-16-1321-2012, 2012.

Andreu, V., Imeson, A. C., and Rubio, J. L.: Temporal changes in soil aggregates and water erosion after a wildfire in a Mediterranean pine forest, Catena, 44, 69–84, doi:10.1016/S0341-8162(00)00177-6, 2001.

Antolín, C.: El sòl com a recurs natural en la Comunitat Valenciana, Consellería de Territorio y Vivienda, Generalitat Valenciana, Valencia (Spain), 1998.

Avendaño Salas, C., Cobo Rayán, R., Gómez Montaña, J., and Sanz Montero, M.: Procedimiento para evaluar la degradación específica (erosión) de cuencas de embalses a partir de los sedimientos acumulados en los mismos. Aplicación al estudio de embalses españoles, Ingeniería Civil, 99, 51–58, 1995.

Avendaño Salas, Ñ., Sanz Montero, M., Cobo Rayán, R., and Gómez Montaña, J.: Sediment yield at Spanish reservoirs and its relationship with the drainage basin area, in: Proceedings of the 19th Symposium of Large Dams, Florence, ICOLD (International Committee on Large Dams), Florence, 863–874, 1997.

Baker, V.: Paleo flood hydrologic techniques for the extension of stream flow records, Transp. Res. Record, 922, 18–23, 1983.

Baker, V.: Paleoflood hydrology and extraordinary flood events, J. Hydrol., 96, 79–99, doi:10.1016/0022-1694(87)90145-4, 1987.

Baker, V.: Paleoflood hydrology: origin, progress, prospects, Geomorphology, 101, 1–13, doi:10.1016/j.geomorph.2008.05.016, 2008.

Bathurst, J. C., Moretti, G., El-Hames, A., Beguería, S., and García-Ruiz, J. M.: Modelling the impact of forest loss on shallow landslide sediment yield, Ijuez river catchment, Spanish Pyrenees, Hydrol. Earth Syst. Sci., 11, 569–583, doi:10.5194/hess-11-569-2007, 2007.

Bellin, N., Vanacker, V., Van Wesemael, B., Solé-Benet, A., and Bakker, M.: Natural and anthropogenic controls on soil erosion in the Internal Betic Cordillera (southeast Spain), Catena, 87, 190–200, doi:10.1016/j.catena.2011.05.022, 2011.

Benito, G.: Palaeohydrological changes in the Mediterranean region during the Late Quaternary, in: Palaeohydrology, Understanding Global Change, edited by: Gregory, K. J. and Benito, G., Wiley, 396 pp., 2003.

Benito, G., Rico, M., Sánchez-Moya, Y., Sopeña, A., Thorndycraft, V. R., and Barriendos M.: The impact of late Holocene climatic variability and land use change on the flood hydrology of the Guadalentín River, southeast Spain, Global Planet. Change, 70, 53–63, doi:10.1016/j.gloplacha.2009.11.007, 2010.

Boix-Fayos, C., De Vente, J., Martínez-Mena, M., Barberá, G., and Castillo, V.: The impact of land use change and check-dams on catchment sediment yield, Hydrol. Process., 22, 4922–4935, doi:10.1002/hyp.7115, 2008.

Brown, C.: Discussion of sedimentation in reservoir, in: Proceedings of the American Society of Civil Engineers, edited by: Witzig, J., Vol. 69, 1493–1500, 1943.

Brune, G. M.: Trap efficiency of reservoirs, T. Am. Geophys. Un., 34, 407–418, 1953.

Camarasa, A. M. and Segura Beltrán, F.: Flood events in Mediterranean ephemeral streams (ramblas) in Valencia region, Spain, Catena, 45, 229–249, doi:10.1016/S0341-8162(01)00146-1, 2001.

Campo, J., Andreu, V., Gimeno-Garcia, E., González, O., and Rubio, J. L.: Occurrence of soil erosion after repeated experimental fires in a Mediterranean environment, Geomorphology, 82, 376–387, doi:10.1016/j.geomorph.2006.05.014, 2006.

Coulthard, T. J., Kirkby, M. J., and Macklin, M. G.: Non-linearity and spatial resolution in a cellular automaton model of a small upland basin, Hydrol. Earth Syst. Sci., 2, 257–264, doi:10.5194/hess-2-257-1998, 1998.

De Vente, J., Poesen, J., and Verstraeten, G.: The application of semi-quantitative methods and reservoir sedimentation rates for the prediction of basin sediment yield in Spain, J. Hydrol., 305, 63–86, doi:10.1016/j.jhydrol.2004.08.030, 2005.

De Vente, J., Poesen, J., Verstraeten, G., Van Rompaey, A., and Govers, G.: Spatially distributed modelling of soil erosion and sediment yield at regional scales in Spain, Global Planet. Change, 60, 393–415, doi:10.1016/j.gloplacha.2007.05.002, 2008.

Title Page

Abstract | Introduction

Conclusions | References

Tables | Figures

|◄ | ►|

◄ | ►

Back | Close

Full Screen / Esc

Printer-friendly Version

Interactive Discussion

Duan, Q., Sorooshian, S., and Gupta, V.: Effective and efficient global optimization for conceptual rainfall-runoff models, Water Resour. Res., 28, 1015–1031, doi:10.1029/91WR02985, 1992.

Duan, Q., Sorooshian, S., and Gupta, V.: Optimal use of the SCE-UA global optimization method for calibrating watershed models, J. Hydrol., 158, 265–284, doi:10.1016/0022-1694(94)90057-4, 1994.

Duck, R. and McManus, J.: Sedimentation in natural and artificial Impoundments: an indicator of evolving climate, land use and dynamic conditions, In: Geomorphology and Sedimentology of Lakes and Reservoirs, edited by: McManus, J. and Duck, R., Wiley, 1993.

Engelund, F. and Hansen, E.: A monograph on sediment transport in alluvial streams, Monogr, Denmark Tech. Univ., Hydraul Lab, 1967.

Foster, I.: Lakes and reservoirs in the sediment delivery system: reconstructing sediment yields, in: Soil Erosion and Sediment Redistribution in River Catchments, Measurement, Modelling and Management, edited by: Owens, P. and Collins, A., Biddles Ltd, King's Lynn, 328 pp., doi:10.1079/9780851990507.0128, 2006.

Foster, I. and Walling, D.: Using reservoir deposits to reconstruct changing sediment yields and sources in the catchment of the Old Mill Reservoir, South Devon, UK, over the past 50 years, Hydrolog. Sci. J., 39, 347–368, doi:10.1080/02626669409492755, 1994.

Francés, F. and Benito, J.: La modelación distribuida con pocos parámetros de las crecidas, Ingeniería del Agua, 2, 7–24, 1995.

Francés, F., Vélez, J. J., Vélez, J. I., and Puricelli, M.: Distributed modelling of large basins for a real time flood forecasting system in Spain, in: Proceedings Second Federal Interagency Hydrologic Modelling Conference, Gan, TY and Biftu, Las Vegas, 3513–3524, 2002.

Francés, F., Vélez, J. I., and Vélez, J. J.: Split-parameter structure for the automatic calibration of distributed hydrological models, J. Hydrol., 332, 226–240, doi:10.1016/j.jhydrol.2006.06.032, 2007.

Gallart, F., Balasch, C., Regüés, D., Soler, M., and Castelltort, X.: Catchment dynamics in a Mediterranean mountain environment: the Vallcebre research basins (South Eastern Pyrenees), II Erosion and sediment dynamics, Catchment dynamics and river processes: latest research with examples from the Mediterranean climate regions, Elsevier, 17–29, 2005.

González-Hidalgo, J. C., Peña-Monné, J. L., and De Luis, M.: A review of daily soil erosion in Western Mediterranean areas, Catena, 71, 193–199, doi:10.1016/j.catena.2007.03.005, 2007.

Sediment yield model implementation

G. Bussi et al.

Full Screen / Esc

Printer-friendly Version

Interactive Discussion

Grauso, S., Fattoruso, G., Crocetti, C., and Montanari, A.: Estimating the suspended sediment yield in a river network by means of geomorphic parameters and regression relationships, Hydrol. Earth Syst. Sci., 12, 177–191, doi:10.5194/hess-12-177-2008, 2008.

Bangqi Hu, Zuosheng Yang, Houjie Wang, Xiaoxia Sun, Naishuang Bi, and Guogang Li: Sedimentation in the Three Gorges Dam and the future trend of Changjiang (Yangtze River) sediment flux to the sea, Hydrol. Earth Syst. Sci., 13, 2253–2264, doi:10.5194/hess-13-2253-2009, 2009.

International Committee on Large Dams (ICOLD): Sedimentation Control of Reservoirs, Guidelines, Vol. 67, 1989.

Johnson, B. E., Julien, P. Y., Molnar, D. K., and Watson, C C.: The two-dimensional upland erosion model CASC2D-SED, J. Am. Water Resour. As., 36, 31–42, doi:10.1111/j.1752-1688.2000.tb04246.x, 2000.

Jolly, J.: A proposed method for accurately calculating sediment yields from reservoir deposition volumes, in: Proceedings of the Exeter Symposium, IAHS Publ. No. 37, 1982.

Julien, P. Y: Erosion and Sedimentation, 1st Edn., Cambridge University Press, 1995.

Julien, P. Y.: Erosion and Sedimentation, 2nd Edn., Cambridge University Press, 2010.

Kilinc, M. and Richardson, E. V.: Mechanics of soil erosion from overland flow generated by simulated rainfall, Hydrology Papers, Colorado State University, 1967.

Kirkby, M., Irvine, B., Jones, R., and Govers G.: The PESERA coarse scale erosion model for Europe, I. Model rationale and implementation, Eur. J. Soil Sci., 59, 1293–1306, doi:10.1111/j.1365-2389.2008.01072.x, 2008.

Kochel, R. and Baker, V.: Paleoflood Hydrology, Science, 215, 353–361, doi:10.1126/science.215.4531.353, 1982.

Lane, E. and V. Koelzer : Density of Sediments Deposited in Reservoirs, Rep. No. 9 of a Study of Methods Used in Measurement and Analysis of Sediment Loads in Streams, 1943.

Le Roux, J. and Roos, Z : The rate of soil erosion in the Wuras Dam catchment calculated from sediments trapped in the dam, Z. Geomorphol., 26, 315–329, 1982.

Machado, M. J., Benito, G., Barriendos, M., and Rodrigo, F. S.: 500 years of rainfall variability and extreme hydrological events in southeastern Spain drylands, J. Arid Environ., 75, 1244–1253, doi:10.1016/j.jaridenv.2011.02.002, 2001.

McManus, J. and Duck, R: Sediment yield estimated from reservoir siltation in the Ochil Hills, Scotland, Earth Surf. Proc. Land., 10, 193–200, doi:10.1002/esp.3290100211, 1985.

Sediment yield model implementation

G. Bussi et al.

Title Page

Abstract | Introduction

Conclusions | References

Tables | Figures

|◄ | ►|

◄ | ►

Back | Close

Full Screen / Esc

Printer-friendly Version

Interactive Discussion

Montoya, J. J.: Desarrollo de un modelo conceptual de producción, transporte y depósito de sedimentos, Ph.D. Thesis, Universitat Politècnica de València (Spain), 2008.

Morales de la Cruz, M. and Francés, F.: Hydrological modelling of the "Sierra de las Minas" in Guatemala, by using a conceptual distributed model and considering the lack of data, WITpress, 97–108, 2008.

Moriasi, D., Arnold, J., Van Liew, M. W., Bingner, R., Harme, R., and Veith, T.: Model evaluation guidelines for systematic quantification of accuracy in watershed simulations, T. ASAE, 50, 885–900, 2007.

Nash, J. E. and Sutcliffe, J. V.: River flow forecasting through conceptual models – Part 1 – a discussion of principles, J. Hydrol., 10, 282–290, doi:10.1016/0022-1694(70)90255-6, 1970.

Nehyba, S., Nývlt., D., Schkade, U., Kirchner, G., and Francu, E.: Depositional rates and dating techniques of modern deposits in the Brno reservoir (Czech Republic) during the last 70 years, J. Paleolimnol., 45, 41–55, doi:10.1007/s10933-010-9478-5, 2011.

Neil, D. and Mazari, R.: Sediment yield mapping using small dam sedimentation surveys, Southern Tablelands, New South Wales, Catena, 20, 13–25, doi:10.1016/0341-8162(93)90026-L, 1993.

Ogden, F. L. and Heilig, A.: Two-dimensional watershed-scale erosion modeling with CASC2D, Landscape Erosion and Evolution Modeling, (RS Harmon and WW Doe III, eds.), Kluwer Academic Publishers, New York, ISBN 0-306-4618-6, 2001.

Phillips, C. J. and Nelson, C. S.: Sedimentation in an artifical lake – Lake Matahina, Bay of Plenty, New. Zeal. J. Mar. Fresh., 15, 459–473, doi:10.1080/00288330.1981.9515938, 1981.

Piest, R. F., Bradford, J. M., and Wyatt, G. M.: Soil erosion and sediment transport from gullies, J. Hydrol. Eng. Div.-ASCE, 101, 65–80, 1975.

Prosser, I. and Williams, L.: The effect of wildfire on runoff and erosion in native Eucalyptus forest, Hydrol. Process., 12, 251–265, doi:10.1002/(sici)1099-1085(199802)12:2<251::aid-hyp574>3.0.co;2-4, 1998.

Roering, J. J., Kirchner, J. W., and Dietrich, W. E.: Evidence for nonlinear, diffusive sediment transport on hillslopes and implications for landscape morphology, Water Resour. Res., 35, 853–870, doi:10.1029/1998WR900090, 1999.

Rojas, R.: GIS-based upland erosion modeling, geovisualization and grid size effects on erosion simulations with CASC2D-SED, Ph.D. Thesis, Colorado State University, 2002.

Romero-Díaz, A., Alonso-Sarriá, F., and Martínez-Lloris, M.: Erosion rates obtained from check-dam sedimentation (SE Spain): a multi-method comparison, Catena, 71, 172–178, doi:10.1016/j.catena.2006.05.011, 2007.

Van Rompaey, A., Verstraeten, G., Van Oost, K., Govers, G., and Poesen, J.: Modelling mean annual sediment yield using a distributed approach, Earth Surf. Proc. Land, 26, 1221–1236, doi:10.1002/esp.275, 2001.

Van Rompaey, A., Vieillefont, V., Jones, R., Montanarella, L., Verstraeten, G., Bazzoffi, P., Dostal, T., Krasa, J., De Vente, J., and Poesen, J.: Validation of soil erosion estimates at European scale, European Soil Bureau Research Report No.13, EUR 20827 EN, Office for Official Publications of the European Communities, Luxembourg, 2003.

Rubio, J. L., Sánchez, J., and Forteza, J.: Proyecto LUCDEM E. Mapa de suelos de la Comunidad Valenciana, 1995.

Rulli, M., Spada, M., Bozzi, S., Bocchiola, D., and Rosso, R.: Modelling sediment yield in burned areas, in: Sediment Budgets: Proceedings of the International Symposium on Sediment Budgets: Held During the Seventh Scientific Assembly of the International Association of Hydrological Sciences (IAHS), edited by: Horowitz, A. and Walling, D., IAHS Publ. No. 292, Foz do Iguaço (Brazil), 162–170, 2005.

Salazar, S., Francés, F., Komma, J., Blume, T., Francke, T., Bronstert, A., and Blöschl, G.: A comparative analysis of the effectiveness of flood management measures based on the concept of "retaining water in the landscape" in different European hydro-climatic regions, Nat. Hazards Earth Syst. Sci., 12, 3287–3306, doi:10.5194/nhess-12-3287-2012, 2012.

Saxton, K. E. and Rawls, W. J.: Soil water characteristic estimates by texture and organic matter for hydrologic solutions, Soil. Sci. Soc. Am. J., 70, 1569–1578, doi:10.2136/sssaj2005.0117, 2006.

Shumm, S. and Lichty, R.: Time, space and causality in geomorphology, Am. J. Sci., 263, 110–119, doi:10.2475/ajs.263.2.110, 1965.

Shakesby, R.: Post-wildfire soil erosion in the Mediterranean: review and future research directions, Earth-Sci. Rev., 105, 71–100, doi:10.1016/j.earscirev.2011.01.001, 2011.

Sougnez, N., Van Wesemael, B., and Vanacker, V.: Low erosion rates measured for steep, sparsely vegetated catchments in southeast Spain, Catena, 84, 1–11, doi:10.1016/j.catena.2010.08.010, 2011.

Title Page

Abstract | Introduction

Conclusions | References

Tables | Figures

|◄ | ►|

◄ | ►

Back | Close

Full Screen / Esc

Printer-friendly Version

Interactive Discussion

Verstraeten, G. and Poesen, J.: Estimating trap efficiency of small reservoirs and ponds: methods and implications for the assessment of sediment yield, Prog. Phys. Geogr., 24, 219–251, doi:10.1177/030913330002400204, 2000.

Verstraeten, G. and Poesen, J.: Modelling the long-term sediment trap efficiency of small ponds, Hydrol. Process., 15, 2797–2819, doi:10.1002/hyp.269, 2001.

Verstraeten, G. and Poesen, J.: Using sediment deposits in small ponds to quantify sediment yield from small catchments: possibilities and limitations, Earth Surf. Proc. Land., 27, 1425–1439, doi:10.1002/esp.439, 2002.

Verstraeten, G., Poesen, J., De Vente, J., and Koninckx, X.: Sediment yield variability in Spain: a quantitative and semiqualitative analysis using reservoir sedimentation rates, Geomorphology, 50, 327–348, doi:10.1016/S0169-555X(02)00220-9, 2003.

Vélez, J. J., Puricelli, M., López Unzu, F., and Francés, F.: Parameter extrapolation to ungauged basins with a hydrological distributed model in a regional framework, Hydrol. Earth Syst. Sci., 13, 229–246, doi:10.5194/hess-13-229-2009, 2009.

Van den Wall Blake, G.: Siltation and soil erosion survey in Zimbabwe, in: Drainage Basin Sediment Delivery, Proceedings of the Albuquerque Symposium, August 1986, edited by: Hadley, R., IAHS Publication 159, 69–80, 1986.

White, P., Labadz, J., and Butcher, D.: Sediment yield estimates from reservoir studies: an appraisal of variability in the southern Pennines of the UK, in: Erosion and Sediment Yield: Global and Regional Perspectives, Proceedings of the Exeter Symposium, July 1996, IAHS Publication 236, Wallingford, IAHS Press, 163–74, 1996.

Wischmeier, W. H. and Smith, D. D.: Predicting rainfall erosion losses-a guide to conservation planning, United States Department of Agriculture (USDA), Washington, DC, USA, 58 pp., 1978.

Discussion Paper | Discussion Paper | Discussion Paper | Discussion Paper | Discussion Paper

Table 1. Flood unit volumes, calculated by two techniques: (i) "wedge" approach: every layer volume was calculated as if each flood unit had a pyramidal shape (such as a wedge); (ii) proportional approach: by subtracting to the actual deposits the average accumulated layer depth, considering the thickness difference of each layer in each trench and approaching it to a pyramidal shape. The "surface gravel body" layer represents the sedimentation produced by multiple events without clear stratigraphic contacts.

Flood unit	Volume (i) (m^3)	Volume (ii) (m^3)
1	34	38
2	8	28
3	172	78
4	10	27
5	14	18
6	55	18
7	22	11
8	20	41
9	195	96
10	153	233
11	75	110
12	8	11
13	37	46
14	30	23
15	18	22
surface gravel body	582	448
total	1434	1248

Title Page

Abstract | Introduction

Conclusions | References

Tables | Figures

◄◄ | ►►

◄ | ►

Back | Close

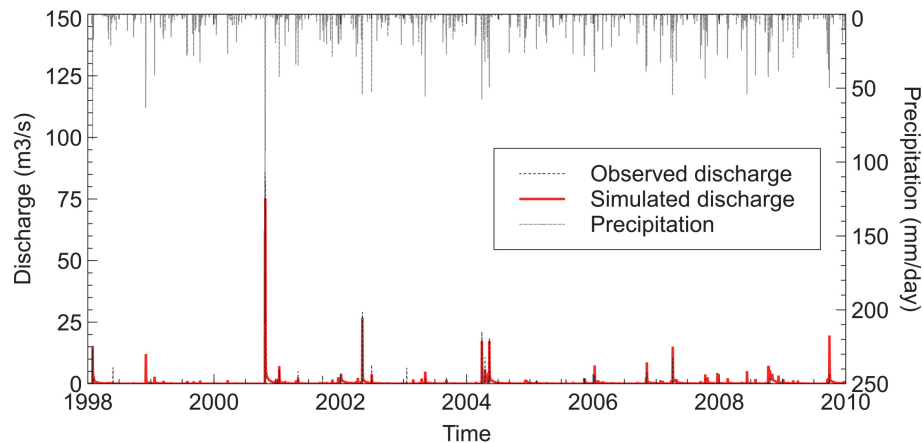Full Screen / Esc

Printer-friendly Version

Interactive Discussion
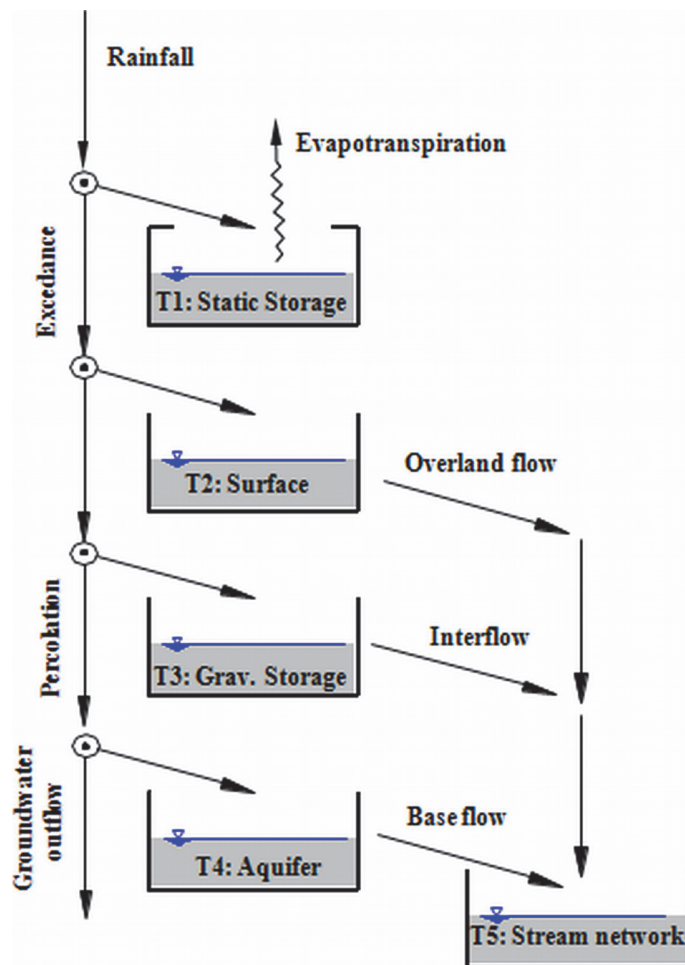
Fig. 1. TETIS hydrological component: vertical conceptual scheme.

Title Page

Abstract | Introduction

Conclusions | References

Tables | Figures

|◄ | ►|

◄ | ►

Back | Close

Full Screen / Esc

Printer-friendly Version

Interactive Discussion
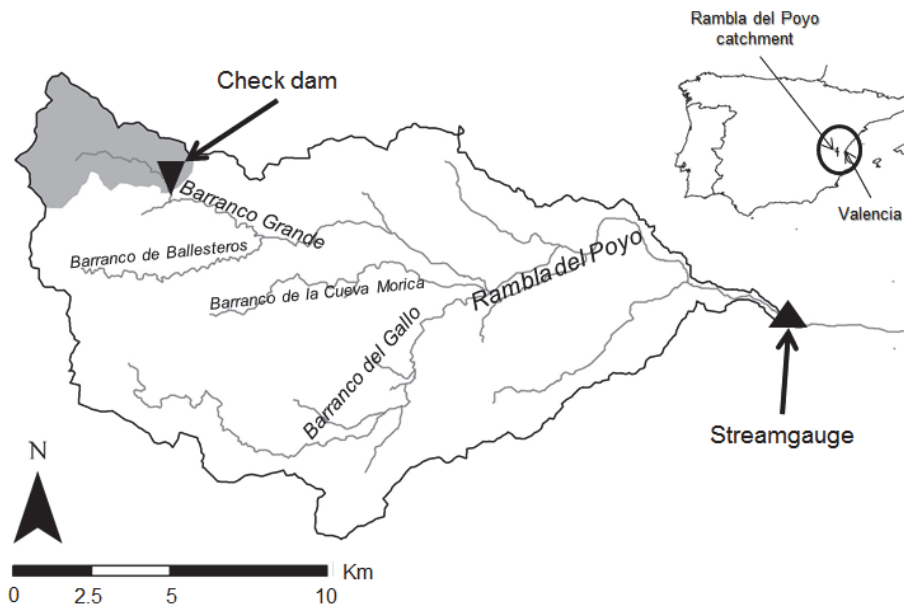
Fig. 2. Location of the catchment. The grey area is the check dam subcatchment.
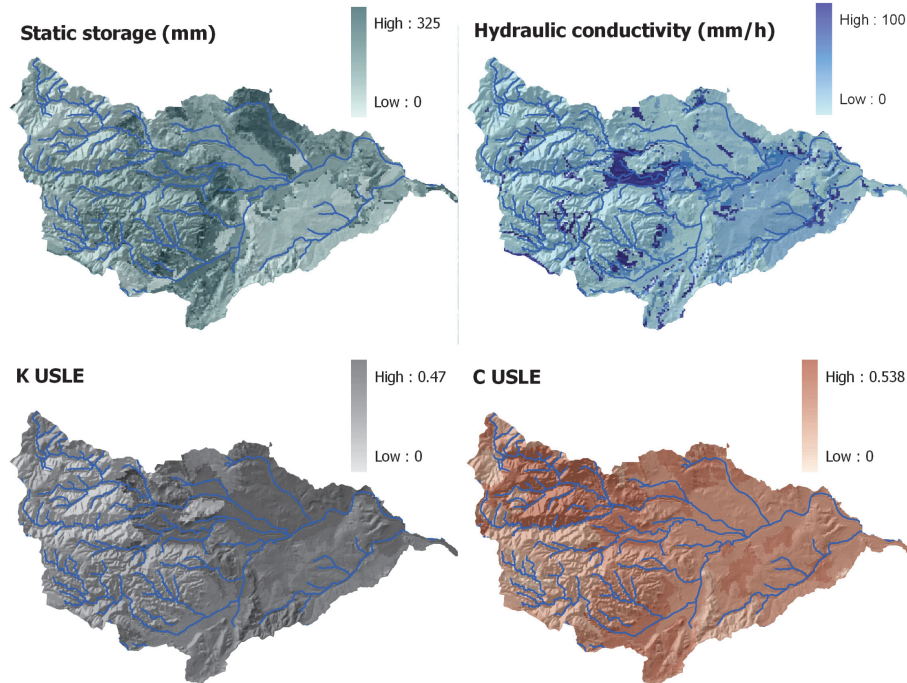
Fig. 3. Maps of the most influent model parameters.

Fig. 4. The check dam.

Full Screen / Esc

Printer-friendly Version

Interactive Discussion

Fig. 5. The reservoir trench BG-1, closest to the dam.

Fig. 6. Hydrological calibration (October 2000 – October 2003) and validation (1998–2010) at daily resolution.
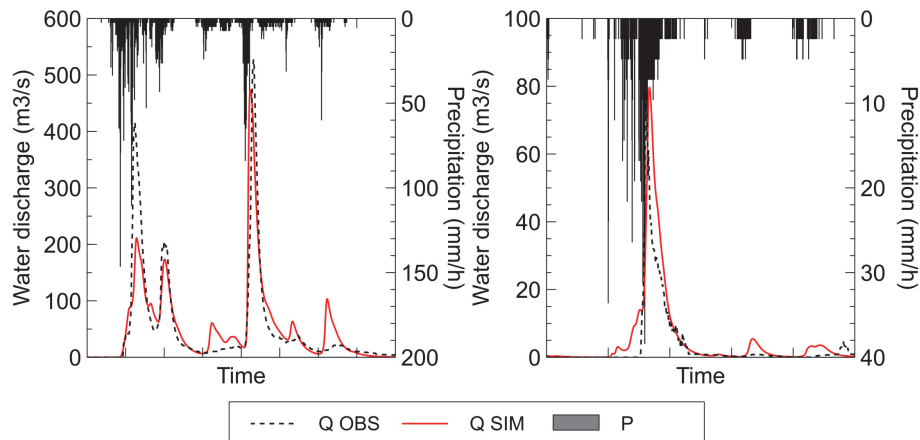
Fig. 7. Hydrological calibration (left) and one of the temporal validations (right) at 5 min resolution.
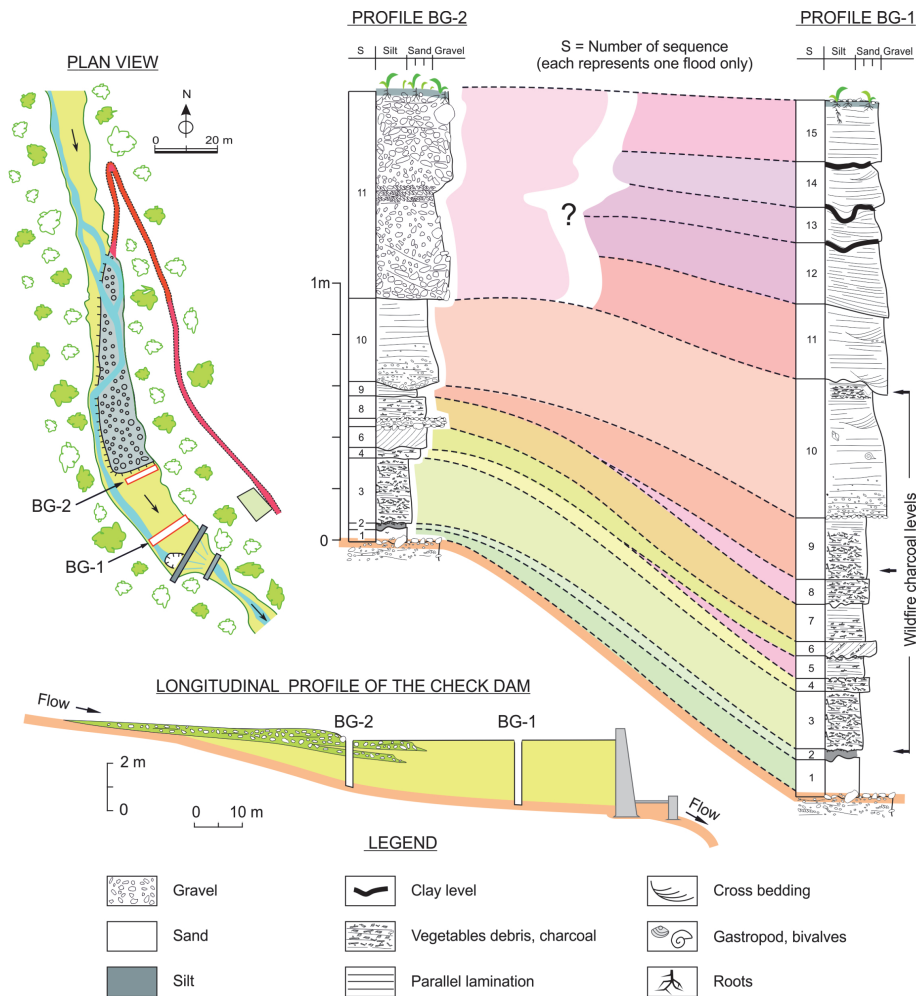
Fig. 8. Partial view of the BG-1 stratigraphic sequence.

Title Page

Abstract | Introduction

Conclusions | References

Tables | Figures

|◀ | ▶|

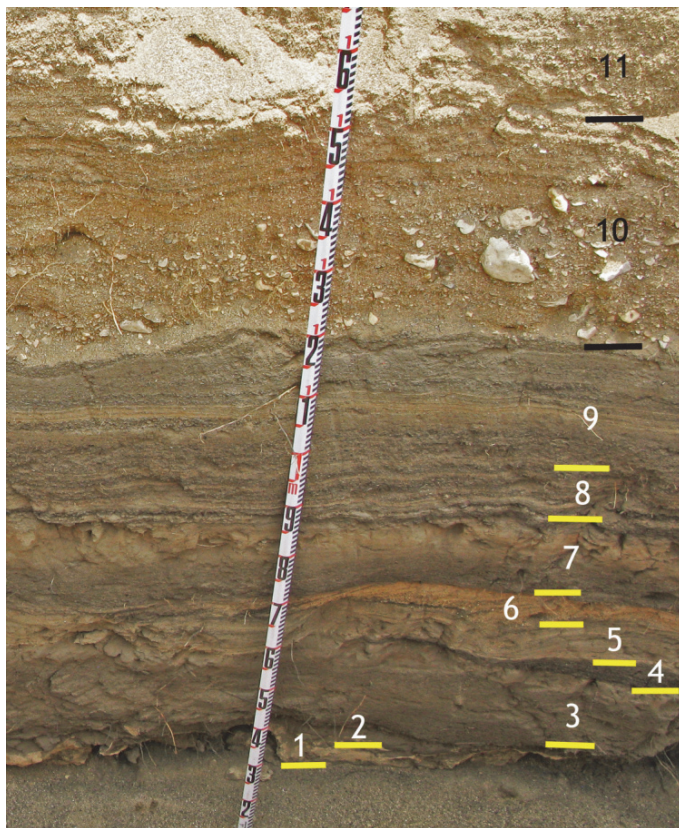◀ | ▶

Back | Close

Full Screen / Esc

Printer-friendly Version

Interactive Discussion

Fig. 9. Upper left: geomorphological sketch with location of the dam structure and trenches BG-1 and BG-2. Bottom left: longitudinal profile across the dam infill and distribution of the two main depositional bodies, i.e. gravel bar and fine deposits (sand and silt). Right: synthetic stratigraphical profiles from trenches BG-1 and BG-2.
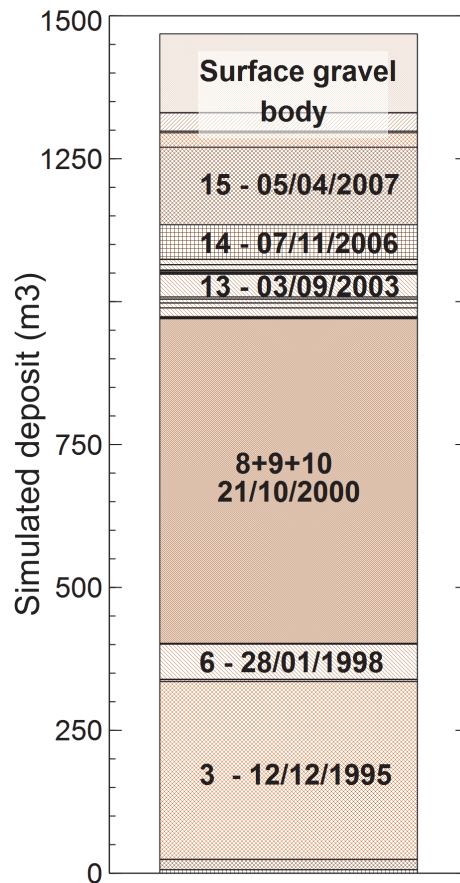
Fig. 10. Simulated deposited volumes with indication of the flood dates (dd/mm/yyyy). The six larger modelled events were assigned to a single or multiple stratigraphic units (numbers preceding the flood date) whose numbers are indicated in Fig. 9. The last three events were assigned to the surface gravel body.

Title Page

Abstract | Introduction

Conclusions | References

Tables | Figures

◄ | ►

◄ | ►

Back | Close

Full Screen / Esc
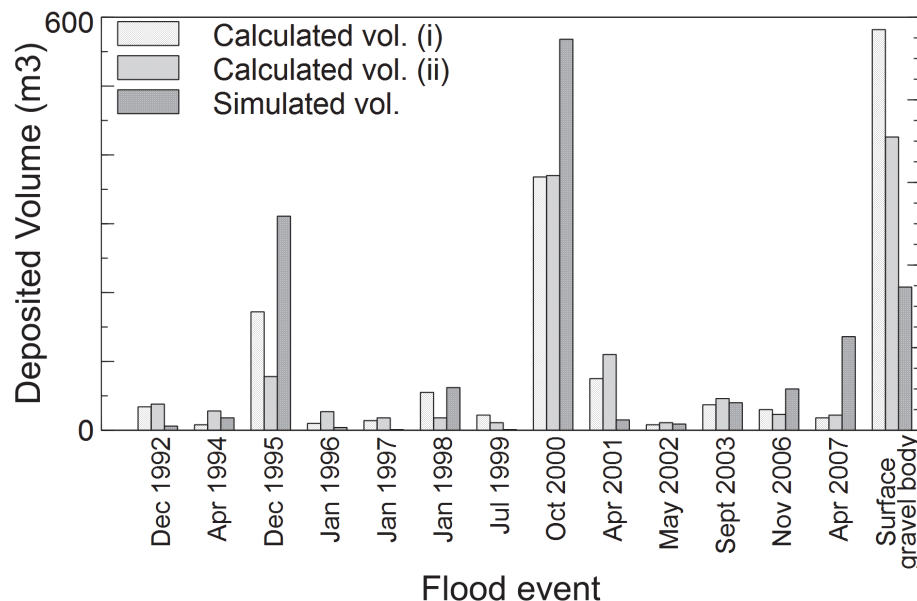
Printer-friendly Version

Interactive Discussion

Fig. 11. Sediment temporal validation (1/2): 13 events (out of 38 modelled flood events) were associated to the 15 detected flood units. The surface gravel body corresponds to the last three modelled events. The model was calibrated using the total sedimentation volume.

Title Page

Abstract | Introduction

Conclusions | References

Tables | Figures

|◄ | ►|

◄ | ►

Back | Close

Full Screen / Esc

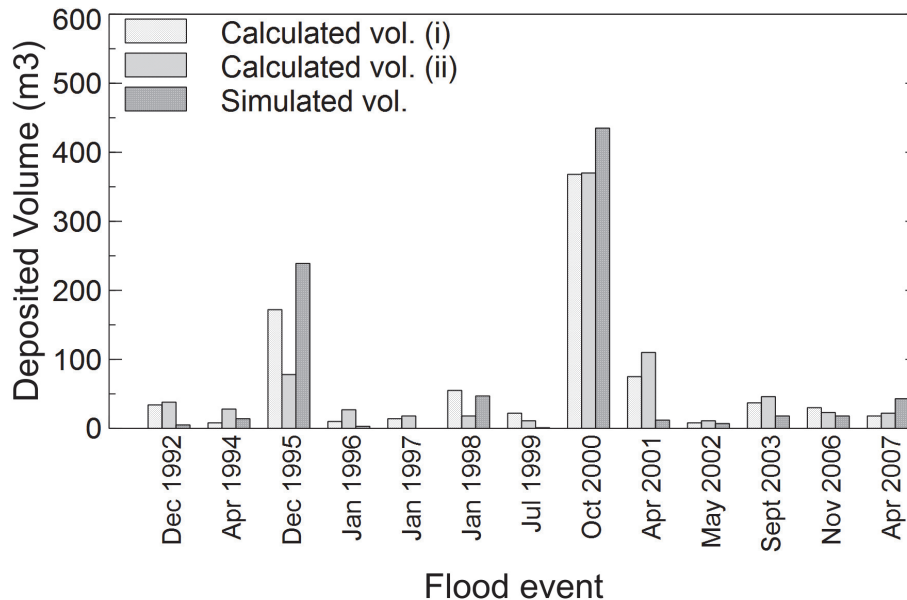Printer-friendly Version

Interactive Discussion

Fig. 12. Sediment temporal validation (2/2): 13 events (out of 38 modelled flood events) were associated to the 15 detected flood units. The surface gravel body was not considered. Notice that model was calibrated using the sum of sedimentation volumes from 1 to 15.